Journal of Environmental Radioactivity 277 (2024) 107462

Contents lists available at ScienceDirect

Journal of Environmental Radioactivity

journal homepage: www.elsevier.com/locate/jenvrad

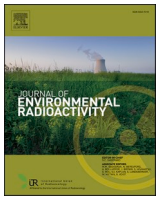

On the detailed mapping of peat (raised bogs) using airborne radiometric data

David Beamish *, James C. White

British Geological Survey, Keyworth, Nottingham, NG12 5GG, UK

ARTICLE INFO

Keywords:
Airborne
Geophysics
Radiometric
Attenuation
Peat mapping
Soil bulk density

ABSTRACT

This study concerns the applied use of the natural radioactivity in soils. The relevance of airborne radiometric (gamma ray) survey data to peat mapping is now well established and such data have been used in a stand-alone sense and as covariates in machine learning algorithms. Here we present a method to use these data to accurately map the boundaries of peat (raised bogs). This has the potential to assist with the estimation of carbon stocks using a property-based assessment of soil. The significance of such regionally-uniform survey data lies in the subsurface information carried by the measurement which contrasts with the surficial nature of many other covariates. Soils attenuate radiometric flux by virtue of their bulk density (and associated carbon content) and water saturation level. The high attenuation levels in low density, wet peat materials give rise to a distinctive soil response. Here an entirely physics-based assessment of flux attenuation is carried out both theoretically and empirically. Radiometric data from the ongoing Tellus airborne survey of Ireland are used. The study area is characterised by an extensive assemblage of discrete raised peat bogs in a framework of largely mineral soils. Peat is detected by a property contrast with adjacent soils and so we consider all soils within the study area. The relatively low lateral resolution of the airborne data is demonstrated by modelling and we examine the behaviour of a combined spatial derivative of the data. The procedure allows the identification of the edges of the 128 peat polygons considered and indicates other additional potential areas of subsurface peat. The data appear to resolve the differences that exist across three available soil/peat databases that are used for the validation of the results obtained.

1. Introduction

Reviewing reports from Intergovernmental Panels on Climate Change, Carsten et al. (2018) note that the amount of organic carbon stored in soils to a depth of 1 m is considered to be about three times that stored in the above ground biomass and twice the amount in the atmosphere. Soil, particularly peat, thus contains highly significant quantities of carbon and presents both opportunities (increased carbon storage) and risks (oxidation and greenhouse gas release) in relation to climate change. Peat also provides other benefits including water storage and filtration, and biodiversity support.

In the context of digital soil mapping, the estimation of carbon content may involve both statistical and, increasingly, predictive (machine learning) approaches. The use of remote sensing data for delineating peatland areas is an important component of making an inventory of peatland carbon stocks which may be estimated when used in combination with covariates (including radiometric data) and with machine learning approaches (Minasny et al., 2019).

There are an increasing number of studies directed at the estimation of both peat and soil parameters in the context of carbon stock assessment. Studies exist at the regional, countrywide and global scales as reviewed by Minasny et al. (2019). Melton et al. (2022) used a machine learning approach in global estimation of peatland extent that incorporated Scottish peat extent data (Aitkenhead and Coull, 2019) and that from Ireland (Connolly and Holden, 2009) as training components for the algorithm. The latter data form part of our study.

Airborne radiometric (gamma ray) data provide a spatially uniform (albeit anisotropic) data set that relates the local scale (e.g. 50–200 m) to regional and, in some cases, countrywide coverage. Reinhardt and Herrmann (2019) provide a critical review of radiometric data applied to soil science (including peat) noting that such data (ground and airborne) not only detect a signal from the landscape surface but integrate information over a certain depth and volume. This is in direct contrast to much remote sensing data (many of which are used as

* Corresponding author.
E-mail addresses: dbe@bgs.ac.uk (D. Beamish), jame3@bgs.ac.uk (J.C. White).

https://doi.org/10.1016/j.jenvrad.2024.107462
Received 21 February 2024; Received in revised form 22 May 2024; Accepted 24 May 2024
Available online 27 May 2024

covariates) which essentially provide purely surficial information. Here we consider the use and limitations of airborne radiometric data in relation to the parameters required in the estimation of subsurface carbon content.

The simplest description of carbon stock estimation, over a certain soil depth interval, would be:

$$\text{Carbon stock (g)} = \text{area (cm}^2\text{) x bulk density (g.cm}^{-3}\text{) x carbon content (\%/100) x thickness (cm)} \quad (1)$$

There are a large number of potential caveats to the simple equation as discussed, for example, by ADAS (2019). As described and developed in the present study, radiometric attenuation by soil is governed by bulk density (BD) and associated soil organic matter (SOM). The attenuation response is also a function of moisture content. In practice, simple rule-of-thumbs (e.g. an average) are often used in estimates in of the thickness of carbon stocks in peat soils (Lindsay, 2010). The potential for mapping peat thickness using airborne data has been studied by a number of authors (e.g. Siemon et al., 2020) but is not considered here. The main utility of the airborne survey data is in relation to the mapping of peat extent (area in equation (1)) which, being a squared term (typically km^2), has more significance than thickness (typically metres in scale) in relation to carbon stock estimation. Our study is intended to provide a framework by which radiometric survey data may be employed in such calculations.

Radiometric data from the ongoing Tellus airborne survey (Young, 2016) across Ireland are used. The Tellus surveys are joint airborne and geochemical surveys with both resource and environmental objectives. An overview of the 30 × 30 km study location is shown in Supplementary Material S1 (Fig. SM1). Existing soil mapping (historical and new) provides a degree of control however inevitable differences in the available databases exist.

The study area is characterised by an extensive patchwork of raised peat bogs (128 polygons) that are an important feature of the central Irish landscape. The bogs are discreet, raised, dome-shaped masses of peat occupying former lakes or shallow depressions. Locally, peat thicknesses can exceed 10 m. The raised bogs are distinct from the Irish upland blanket bogs previously studied by Beamish (2013, 2016a). These studies together with those across lowland areas (meres, fens and afforested peat) and upland areas of blanket peat (Beamish, 2014a) form an existing framework of airborne radiometric attenuation assessment applied to peat.

Bedrock lithologies (the radiometric source) may change across the study area. Potentially each lithological unit encountered can provide a distinct radiometric response (considered primordial) in terms of the 3 main radionuclides (Potassium, Thorium and Uranium) and their ratios which, together with the total flux, can modify the observed response. The observed distinctions form the basis for geological exploration. When considering attenuation, a spatial joint assessment of both soil and bedrock is normally required (Beamish and White, 2011; Beamish, 2013). The present study area was, in part, chosen because the bedrock is entirely composed of various Lower Carboniferous limestone lithologies. We are of the opinion that the variability of the attenuation response levels presented here are entirely soil related.

Due to the highly technical nature of airborne radiometric data, and since such data may be used as covariates by the non-specialist, a theoretical framework is provided. This contains a theoretical modelling of the characteristics of the spatial behaviour of flux, at the appropriate survey altitude, across an idealised peat bog. The use of a spatial derivative (the horizontal gradient magnitude, HGM) to detect the edges of the bog is demonstrated. The mapping of peat obtained using the HGM response together with the attenuation characteristics of the data is evaluated using both detailed studies (individual bogs) and at a regional scale. An assessment of the accuracy of the results obtained is limited by differences that exist across the three control peat databases used. Our results appear to resolve such ambiguities. Many new areas of potential peat are also identified. The principal objective of our study is to demonstrate the detailed mapping of peat boundaries at both local and regional scales.

2. Theoretical framework

Peat is a soil characterised by its relatively high organic matter content, which may range from 30% to almost 100% (Lindsay, 2010). Peat is formed from carbon rich, dead and decaying plant material, which has accumulated in waterlogged conditions over thousands of years. Peat has a very low mineral content; therefore, it is much less dense than other soil materials, and most of its volume is occupied by water when wet. Soils with peat layers generally have dry bulk densities ranging from 0.06 g.cm^{-3} to 0.25 g.cm^{-3} depending on the level of humification, compaction or mineral content (Kiely et al., 2009; JNCC, 2011). The typical carbon content of peat is approximately 52% carbon by dry weight (Lindsay, 2010).

The conceptual model of radiometric flux attenuation was previously discussed by Beamish (2013, 2015). It is assumed that bedrock material acts as a geochemical and radionuclide parent to any derived (overlying) superficial (i.e. unconsolidated) sediments and soils. The bedrock is considered to provide the primary radiometric response. The at-surface soil material is then considered to possess a specific and locally uniform radionuclide concentration that derives from the underlying parent material (in the absence of transport effects). The soil, where present, attenuates the observed (in-air) gamma-ray flux primarily through density when the material is dry (Løvborg, 1984). Additional secondary attenuation effects are introduced when the material contains free or absorbed water (Grasty, 1997), as described later.

In addition to the role of the soil parent material (bedrock) we should also note the differing origins of radioactivity in organic soils and in raised bogs, in particular. This stems from the potential hydrogeological isolation of raised bogs which is a required component in their formation (Cross, 1990). Lidman et al. (2013) discuss the general origins of radioactivity in peat. In the case of raised bogs the domed profile of an intact raised bog ensures that it will be ombrotrophic, i.e. it relies on precipitation for water content.

Much of the literature on the radiometric content of soils concerns their uptake by biota (e.g. Tamponnet et al., 2008). Here we take a more pragmatic approach and consider observational soil measurements of radionuclide concentrations. We use the associated ground-based geochemical survey of soil, stream water and stream sediment data incorporated into all the Tellus programmes thus far. The soil geochemical surveys provide upper (>5 cm) and lower (>50 cm) soil analyses of over 50 major and trace elements and include sampled concentrations of the 3 main radionuclides. The upper soil results for the initial 2 Irish surveys covering Northern Ireland and the Border counties of the Republic of Northern Ireland are presented and discussed by Gallagher et al. (2006). Sampling was based solely on uniform spatial sampling densities (e.g. 1 sample per 2 km^2) giving rise to 10,355 data points. Discussion of the results is primarily focused on the differing bedrock controls of the soil radionuclide concentrations but the authors also provide summary statements with regard to the observed non-peat and 'peaty' top soil variations; their results for topsoil (5–20 cm) are now summarised.

In the case of Potassium, non-peaty topsoil had a median concentration of 0.13% compared to 0.06% in peaty topsoil (a reduction factor of 2.17). For Thorium, non-peaty topsoil had a median concentration of 2.2 mg kg^{-1} compared to 0.7 mg kg^{-1} in peaty topsoil (a reduction factor of 3.14). For Uranium, non-peaty topsoil had a median concentration of 1.03 mg kg^{-1} compared to 0.49 mg kg^{-1} in peaty topsoil (a reduction factor of 2.10). The results obviously apply to all the bedrock types as discussed by Gallagher et al. (2006) but also all the differing forms of peat encountered (e.g. upland blanket bogs, lowland fens and lowland raised bogs).

Thus, in addition to the soil attenuation factors discussed below, it is

possible that peat areas contain reduced radionuclide concentrations in relation to their mineral soil counterparts (by the factors suggested above). In reality, there are likely to be many factors involved in the detailed variation of radionuclides within soils (see for example Lidman et al., 2013). Although coarsely sampled, more controlled studies of the Tellus geochemistry data with regard to their soil and bedrock classifications are recommended. Comparisons between the ground geochemical soil sampling and the airborne data were undertaken for the Northern Ireland Tellus project by Beamish (2014b).

2.1. Vertical resolution and attenuation

The attenuation behaviour of various soils (and water), are shown in Fig. 1a using a logarithmic ordinate. We use generic values for different soil types suggested in the literature and discussed by Beamish (2013) who also notes other relevant details. The calculation assumes a vertically uniform material and ignores the spatially cumulative nature of the response discussed later. The mineral soil parameters use typical limiting densities of 1.1 and 1.6 g. cm^{-3} and both use porosities of 40% and a water saturation of 40%. The water density is 1 g. cm^{-3}. Parameters for the 2 peat soils are obtained from the 'standard' Clymo (1992) peat (bog) model with an acrotelm (active plant) layer above the more compact catotelm (humic) material. Lindsay (2010) discusses the Clymo model in detail. Detailed studies of bogs adjacent to the study area indicate the acrotelm thickness may extend from 0 to 50 cm (Heggeler et al., 2005). Here we assign typical peat porosities and water saturations of 90%. In order to provide a high-density limiting case Fig. 1 shows the behaviour of a bedrock outcrop of limestone. A 'dry peat' result is also shown here using a 50% saturation indicating that degraded and cutover bogs (or portions thereof) may give rise to variable attenuation lengths depending on any reduced saturation levels. It is worth noting that radiometric attenuation is necessarily defined as a relative change in count rate (radiometric flux) so that here, as previously, attenuation is referenced to a material of the same bulk density with no water content.

If we use a 90% reference attenuation level to obtain a realistic 'depth of investigation' for the majority of soils we obtain vertical scales of between 40 and 55 cm. Indicative soil depths in the study area are largely >80 cm (Creamer et al., 2016; Creamer and O'Sullivan, 2018). The behaviour of the same soils in relation to degree of saturation is shown in Fig. 1b. An additional peat response using a density of 0.25 g. cm^{-3} denotes the approximate limiting case for 'peaty' soils (Kiely et al., 2009). It is clear that attenuation in the low density peat and 'peaty' materials is totally distinct from the higher density mineral soils for all realistic soil saturations. The behaviour forms the main basis for the detection of peat materials using radiometric attenuation.

2.2. Field of view (FOV): the volumetric footprint

Generally, spatial integration in both the above and below ground volume of a measurement is intrinsic to many geophysical instruments as discussed by Köhli et al. (2015). In order to assess the volume of material contributing to the gamma-ray flux measured by an airborne detector, Duval et al. (1971) introduced the concept of a circle of investigation (field of view, FOV). The authors performed theoretical calculations based on a flat homogenous material that is infinitely large and infinitely thick (the so-called infinite source). Pitkin and Duval (1980) subsequently considered the broader design requirements of airborne surveys in terms of their resolution capabilities. The field of view increases with the height of the detector and the behaviour was summarised by Beamish (2016b) using the lower flying heights of modern surveys. Fig. 2a shows the spatial scale of the cumulative contributions for a survey height of 75 m, across 3 flight lines (200 m spacing). This is a cross-section through the radially symmetric isovolume of contributions. The height chosen is commensurate with the mean survey heights across the study area. We note that a 50% contribution is only achieved over a distance approaching 100 m. The 90% contribution extends towards 300 m. A similar graphic for a flying height of 125 m is presented by Fortin et al. (2017); at the increased altitude, the 90% contribution extends to a circular diameter of 509 m. As noted later, certain portions of the data across the study area were acquired at elevations >150 m.

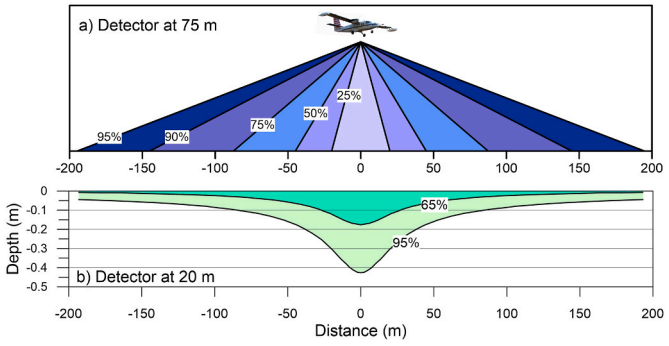

Fig. 2. Field of view (FOV) of an airborne measurement. Not true scale. (a) Detector at 75 m (aircraft), percentage radial contributions to the measurement. (b) Detector at 20 m (drone), after van der Veeke et al. (2021), subsurface contributions (65% and 95%) to the measurement.

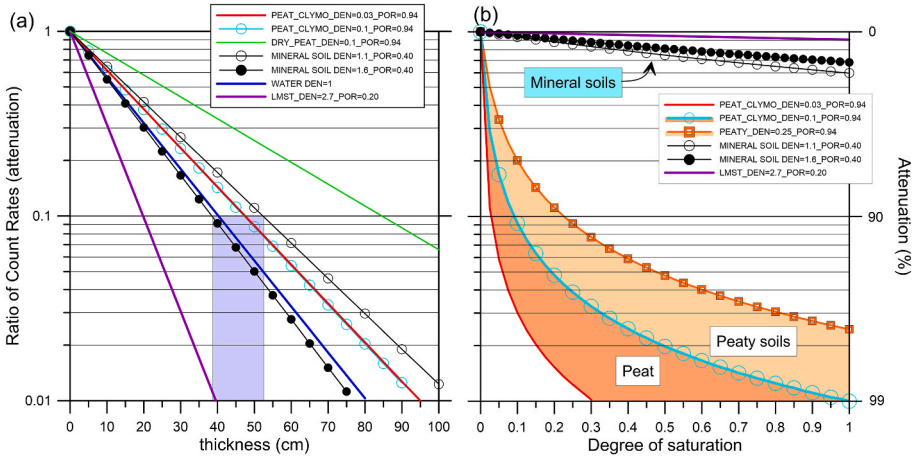

Fig. 1. Theoretical attenuation behaviour of vertically uniform soil/bedrock types. The parameters defining the soil types are discussed in the text and noted in the legend (DEN: Density, POR: Porosity, LMST: Limestone). (a) Attenuation as a function of thickness (depth). (b) Attenuation as a function of fractional saturation.

Duval et al. (1971) refer to the subsurface contribution to the observed flux as 'dish-shaped'. Van der Veeke et al. (2021) revisited and extended the calculations of Duval et al. (1971) in relation to the lower altitudes used in drone surveys. The authors assess a maximum angle where the attenuation through the air is equal to the attenuation through the ground and air directly beneath the detector. This provides an isovolume of the subsurface contributions describing their spatial behaviour. Fig. 2b shows a cross-section of the 65% and 95% contributions reproduced from the results presented by Van der Veeke et al. (2021) for a drone sensor altitude of 20 m (the maximum altitude considered). It is used here for illustrative, rather than quantitative, purposes. At greater altitudes the isovolume will increase in scale but the general 'dish' form should be maintained. The largest fraction of detected flux will originate from the deeper volume centred beneath the observation point. In essence, the radiometric volumetric response at an observation point derives from a very large 'thin dish'. Each airborne observation is radially cumulative around the central sampling point with both deep and shallow depth contributions from the soil.

2.3. Modelling the radiometric response of a peat bog

Of most relevance to survey data is the response behaviour when non-uniform distributions of radioactivity are encountered. The model considered here is a finite area source (e.g. a circle or linear strip) defined by a relative increase/decrease in source concentration. The change in concentration is used to simulate the change in flux across the anomalous region. Duval (1997) produced a United States Geological Survey report, providing and describing, a set of gamma-ray modelling programmes that are based on previous publications. Beamish (2016b) used the software to provide a spatial analysis of airborne data with a survey elevation range from 60 to 120 m. Circular anomalous (enhanced concentration) regions with radii between 25 and 200 m were studied. Bell-shaped responses were observed with the correct source concentration (and hence flux) only approached at a source radius of 200 m (60 m elevation). As the radius increases the observed flux becomes constant (at the correct amplitude) across the centre of the source. Since the definition and hence spatial resolution of the source area was low, Beamish (2016b) assessed the use of the horizontal gradient magnitude to enhance the 'edge-detection' capabilities of the data. Both theoretical (model) and empirical (survey) data were considered.

For gridded data the total horizontal gradient magnitude (HGM) is based on the x-derivative (dx) and y-derivative (dy) responses and is defined as the positive-only response:

$$HGM = \sqrt{(dx)^2 + (dy)^2} \quad (4)$$

The calculation will amplify the noise content of a particular data set and it is relevant to consider the signal to noise characteristics of the data.

Here we present the modelling of an isolated peat bog. We use an anomalous region of width 500 m and a reduction in radioactivity concentration of 50 to simulate the flux attenuation. Both an infinite linear source (a perpendicular profile) and a circle (radius of 250 m) are considered. The elevation used is 75 m together with a soil density of 1 g. cm^{-3}. Fig. 3 shows the flux data (left ordinate) and calculated HGM (right ordinate) across a profile distance of 1 km. The flux data for both bodies display similar, bell-shaped attenuation behaviour (a characteristic response of the measurement) and return to the correct background level some ~250 m beyond the body edge. The behaviour can be termed a lateral edge adjustment distance (of flux) due to the 2D/3D nature of a zone of discrete flux attenuation. There are 2 edge adjustment distances, one internal, and one external to the body edge. When, as here, sharp high contrasts in soil bulk density occur (e.g. between Brown Earth and peat soils) a significant adjustment 'halo' is produced in flux amplitude.

The HGM response of the infinite linear source produces a slightly larger peak response at the body edge and is located precisely at the boundary. The HGM peak of the circular source appears to lie just within the source boundary and it is possible to speculate that this may be effect of the source edge curvature of the idealised model circle. For larger bodies the radiometric response is uniform over the source region and produces no horizontal gradient. Horizontal gradients are then produced across the edges in accord with those observed in Fig. 3. When considering a grid of HGM estimates, Beamish (2016b) also demonstrated a common processing procedure to extract the maxima of the HGM response as described by Phillips et al. (2007). These authors employed a 3 × 3 (grid cell) moving-window to assess the local curvature and define turning points. Here we use a ridge analysis (also referred to as curvature-analysis) to isolate maxima in the HGM response across our study area. Being a grid-based procedure, the ridge estimates are obtained at the grid resolution. Essentially the procedure provides an edge-detection method in relation to significant contrasts in soil properties (e.g. boundaries of peat zones) within the data set.

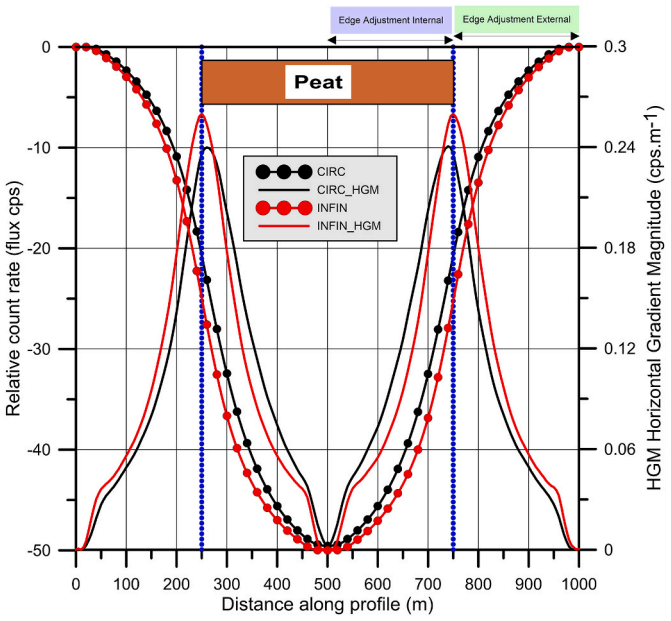

Fig. 3. Attenuation cross-section across a model peat bog (250–500 m) with a reduction in source concentration in radioactivity of 50. The results are obtained for a circular (CIRC) and an infinite strip (INFIN) source body. Also shown (right ordinate) are the magnitudes of the associated Horizontal Gradient Magnitudes (HGM).

The characteristic response shown in Fig. 3 is retained for all concentrations of the body but the amplitude reduces with decreasing concentration. The calculated HGM response then behaves in a corresponding manner. The amplitude of the HGM response can then be used to infer the level of the change in concentration across body edges. It is worth noting that the modelled bog edge is idealised and, in reality, may be gradational. Graphics showing the sequential Holocene development of the originally hydrogeologically-isolated bog structures are available (Cross, 1990; Heggeler et al., 2005) but these are idealised. More relevant detailed edge information can be found in Howie and Meerveld (2011). Lidman et al. (2013) present a detailed study of radionuclide concentrations across the edge of a single bog indicating the variations measured over a distance scale of only 10 m. Given the intrinsic resolution of the data, 60 m along-line with lines 200 m apart, it is unlikely that any precise gradational edge variations in concentration can be detected.

3. Materials and methods

A 30 × 30 km regional study area (Fig. SM1) was selected across the central Irish Midlands which is an area characterised by an extensive

patchwork of raised peat bogs. The advantage of assessing such bogs is that they present laterally confined areas, at a wide range of scales, which permit a detailed assessment of the resolution capabilities of the airborne data. The two main soils types encountered are mineral (Brown Earths, 55% by area) and peat (32% by area). The data and presentations all use coordinates in the IRENE95 datum, Irish Transverse Mercator (ITM) projection (EPSG:2157).

3.1. Tellus airborne radiometric data

The Tellus Irish national programme managed by Geological Survey of Ireland (GSI) involves (a) an airborne geophysical survey using multiple sensors and (b) a ground-based geochemical survey of soil, stream water and stream sediment. This study primarily makes use of (a) but (b) is also referenced. The airborne data are acquired across individual survey blocks that result from year-on-year surveying across Ireland (with winter breaks). Certain survey specifications remain constant. The survey line direction is 165/345° with lines spaced at 200 m intervals. The nominal, regulatory survey altitude is largely 60 m except for one block acquired at 90 m. Survey altitudes are required to increase over conurbations and some fixed structures (e.g. wind farms). The surveys specified a 60 m/s constant velocity and so a ~60 m ground sampling was largely achieved.

The radiometric data are recorded by a spectrometer covering the 0.3–3 MeV energy range with the spectrum sampled at 1 s intervals. Both 256 and 1024-channel systems have been employed. The 4 surveys used here (Fig. SM1) employed an Exploranium GR820 (Blocks A1 and TNM) and a Radiation Solutions RS-501 (Blocks A2 and A5). The older Exploranium spectrometer system includes an on-board computer for real-time signal processing and analysis, allowing automatic gain control for individual crystals using the natural thorium peak, and multi-channel recording and analysis. The system utilizes a NaI(Tl) total detector volume of 63.0 L consisting of 12 downward-looking and 3 upward-looking parallelepiped crystals of 4.2 L each, housed in three detector packs. The data were recorded in 256 channel spectral mode and windowed data mode at an interval of 1 Hz. The Radiation Solutions spectrometer system is similar allowing automatic gain control for individual crystals using the natural thorium peak, and multi-channel recording. In this case the system again uses crystals of 4.2 L with 16 downward-looking and 3 upward-looking NaI(Tl) crystals giving a downward volume of 67.2 L and upward volume of 12.6 L. Data were recorded in 1024 channel spectral mode and windowed data mode at an interval of 1 s.

Comprehensive information on both the instrumentation, calibrations and processing procedures are given in the contractors reports which can be found on the Tellus project website (www.tellus.ie). The reports are accessible from the geophysics page (within the project landing page, as above). As a specific example, the technical report for Block A1 can be found at https://gsi.geodata.gov.ie/downloads/Tellus/SGL_Tech_Report_831A2_000.pdf.

The spectral ranges of the estimated radionuclides and total count are given in Table 1. The mass attenuation coefficients are from Billings and Hovgaard (1999).

Table 1
Spectral energy ranges of the airborne radiometric data.

Window	Nuclide	Energy range (MeV)	Mass Attenuation Coefficient in soil cm^2/g
Thorium (eTh)	^{208}Tl (2.61 MeV)	2.41–2.81	0.0396
Uranium (eU)	^{214}Bi (1.76 MeV)	1.65–1.86	0.0482
Potassium (% K)	^{40}K (1.46 MeV)	1.37–1.57	0.0528
Total Count (cps)	–	0.40–2.81	–

Data calibration and processing uses well-established guidelines and procedures given in Grasty and Minty (1995) and IAEA (2003). The processing provides calibrated values of radiometric flux in counts per second (cps) across the energy ranges shown in Table 1. Conventionally the airborne flux values are converted to equivalent ground concentrations (eTh, eU assuming secular equilibrium in the decay chains) by multiplying the estimated radionuclide flux values by a calibration constant determined across a calibration range for each survey (IAEA, 2010). The 'line-based' radiometric survey data (in the form of a database) have been made available in 2 forms on the Tellus project website (www.tellus.ie) the project landing page. The data are accessible from the geophysics page (within the project landing page).

Data Release A. Data were obtained from individual survey blocks that result from year-on-year surveying across Ireland (with winter breaks). The processing, calibration and delivery of these data are described in the contractor reports associated with each survey block. The overlapping survey blocks are illustrated in Supplementary Material (Fig. SM1).

Data Release B. Data were merged by the GSI across a set of blocks to obtain a seamless and spatially continuous database. The procedure uses the mean values (from gridded data) in survey overlap areas to determine a correction factor for each radionuclide and for each survey block. Here we examine the merged line-data from Tellus 2019B (Merged areas of Tellus phases). The data release contains the data and an associated geophysical technical report and data release notes.

Equivalent data from both deliveries A and B were examined/compared across the study area. It is clear that the 2019B merged data (Data Release B) present a smoothed version of the original survey data. As a consequence, line data from Data Release A with 50 m grids obtained using minimum curvature are used to achieve the maximum spatial resolution.

3.2. Soils (TEAGASC)

The main soil database used here derives from the Teagasc-EPA Soils and Subsoils Mapping Project (Fealy et al., 2009). This is available at https://gis.epa.ie/GetData/Download. The soils database derives, in part, from a National Soils Survey initiated in 1959 but later work involved a framework taking in both the Quaternary and bedrock (parent material). A software-based expert classification system provided predictive modelling to produce the final, indicative soil map. The map classifies the soils of Ireland into 25 classes at a nominal working scale of 1:100,000 to 1:150,000. The peat classification scheme within this framework is described by Connolly et al. (2007) and Connolly and Holden (2009). The classifications are described as qualitative and include a binary depth qualifier. It is very important to note that the depth qualifier used is indicative. The class 'shallow' was assigned to soils that overlay subsoil classes perceived to supply a shallow soil-formational environment. These Quaternary classes include eskers, gravels and rock outcrop/subcrop. The latter are only associated with non-peat soils. All other soils occurring on tills (the majority) are given the qualifier 'deep'. Efforts were made to recognise the fringes of larger bogs which have been reclaimed for agriculture. The centuries old practice of reclamation or 'marling' of peat bogs is described by Hammond (1979) and typically involved the addition of calcareous glacial tills/gravels to the topsoil and the introduction/modification of drainage. The mineral materials introduced into the upper soil horizon would clearly increase bulk density and it is likely that such effects are present in the study area.

The full classification of soils across the study area contains a number of zero or very small classes. Here we use a simplification (grouping) of the main classes present in our study area as shown in Table 2.

All peats within the study area are classed as raised bog (basin) and as cutaway/cutover acknowledging that all the bogs have been subjected to various levels of peat extraction. Peat within some of the larger bogs was industrially harvested at the time of the surveys but this

Table 2
Simplified 6-category TEAGASC soil classification scheme showing code used here (A to F) for the 30 × 30 km study area. IFS refers to the Irish Forestry Soils coding in the TEAGASC database.

Code	Description	IFS Code	Examples	% Area
A	Deep and shallow well-drained mineral	12, 22	Brown Earths, Lithosols	46.0
B	Deep and shallow poorly-drained mineral	31, 32, 34	Brown Earths, Gleys	8.6
C	Poorly drained mineral with peaty topsoil	42, 44, 45	Peaty Gleys	2.4
D	Shallow lithosolic potentially with peaty topsoil	46	Lithosols, Peats	2.5
E	Alluvium	51, 53	Mineral, Marl	7.0
F	Cutaway/cutover peat	65	Raised bog	31.7

activity has since ceased. Many of the bogs in the study area have protected status and may be designated Special Areas of Conservation (SAC) or Natural Heritage Areas (NHA) (Mackin et al., 2017). These are described by the National Parks & Wildlife Service (https://www.npws.ie/protected-sites). Conservation objectives and notes for some of the protected bog sites can be obtained from the service.

The simplified (6 soil classes + made ground) version of the Teagasc soil map is shown in Fig. 4. Well drained Brown Earths (class A) are the most extensive soil group accounting for 46% of the study area and these are followed by cutover Peat (class F) at 32%. The remaining groups account for less than 10% each. The 2 main groups offer high contrast zones in terms of their bulk density. Organo-mineral soils (classes C and D) are limited in occurrence (5% by area) and are of limited use for an overview assessment.

3.3. Quaternary (superficial) deposits

The Quaternary deposits map across the study area is included in Supplementary Material (Fig. SM2). The main types of sediment recognised are tills, glacio-fluvial/lacustrine deposits, alluvium, lacustrine sediments and peat. Corings through various peat bogs to bedrock reveal the variability of the materials underlying the peat (e.g. Smyth, 1992). Raised bogs, due to their genesis, are typically underlain by a lacustrine clay layer. The Quaternary database classification of cutover raised peat allows a further assessment of peat mapping across the study area. The Quaternary data are available digitally from the Geological Survey of Ireland (https://www.gsi.ie/) and have a nominal scale of 1:50k.

3.4. Bedrock

The bedrock map across the study area is included in Supplementary Material (Fig. SM3). In the case of the present study area the bedrock is entirely composed of various Carboniferous limestone lithologies. The two main lithologies are dark limestone and shale (calp) and massive unbedded lime-mudstone. The bedrock database is available digitally from the Geological Survey of Ireland (https://www.gsi.ie/) and here we use a mapping scale of 1:100k (the 2018 map).

3.5. CORINE land classification database (CLC18)

To further define peat variability in terms of land classification, CORINE (Coordination of Information on the Environment) data were used. The database comprises an inventory of land cover in 44 classes and is produced by visual interpretation of high-resolution satellite imagery. Here we use CLC2018 (available from https://land.copernicus.eu/sitemap) and refer to the land-classification code of 412 which describes peat bog.

3.6. Lidar data

Small clusters of public-domain topographic Lidar data are available across the study area. Here, a single example is used to illustrate the nature of the highly modified surface of a cutover peat bog. Digital Elevation Models (bare earth) rasters were obtained from the Open Topographic Lidar Data page of the Government of Ireland website (https://data.gov.ie/dataset/open-topographic-lidar-data). The rasters used have a resolution of 2 × 2 m and are dated as 2011.

3.7. The study area

Fig. 5a shows the large-scale topography across the study area which is centred on the river valley of the Shannon. Surface elevations were obtained from the NASA's Shuttle Radar Topography Mission (SRTM) Global 1 arc-second (30 m) DEM. The study area contains part of the alluvial Middle Shannon connecting Lough Ree in the NE (beyond the study area) to Lough Derg (a flow-through lake) in the SW of the study area. The river is a low gradient, low energy system. The valley is characterised by a floodplain and adjacent seasonally flooded areas called callows.

Fig. 5 a,b show the Teagasc soil areas mapped/classified as raised peat bog in transparent grey. These areas occur at all scales and across all topographic levels from smaller clusters on the high ground in the

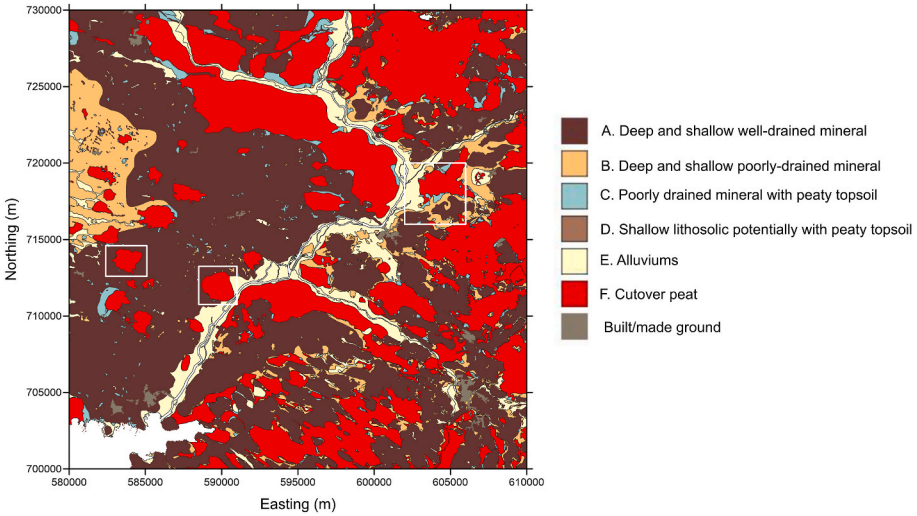

Fig. 4. The simplified version of the TEAGASC soil map (see Table 2), with the addition of made/built ground in grey. 3 white rectangles are identified in Fig. 5.

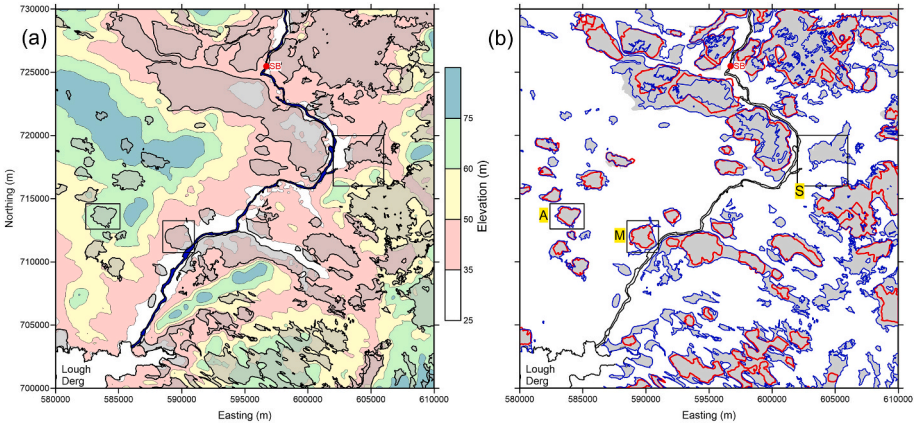

Fig. 5. The 30 × 30 km study area centred on the Shannon river (blue). SB=Shannonbridge. (a) Large scale topography with Teagasc soil mapping of peat areas shown in transparent grey. (b) 3 databases providing mapping of peat areas (i) Teagasc shown in grey infill, (ii) Corine CLC18 mapping of peat shown in red line and (iii) Quaternary mapping of peat shown in blue line. The 3 rectangles denote detailed study areas, A = Ardraigue Bog, M = Meeneen Bog, SH=Shannon Harbour. (For interpretation of the references to colour in this figure legend, the reader is referred to the Web version of this article.)

west to more extensive areas showing a degree of association with the river valley. The lowest elevation contour interval (25–35 m), defining much of the floodplain of the Shannon, can also be observed within some of the larger bogs.

As discussed above, there are 3 peat databases that can be examined to assess the accuracy of the geophysical spatial assessment of peat. The first two are mapping products (the Teagasc soils database and the GSI Quaternary database) while the third is a satellite based optical product (Corine CLC18). These are now compared. Fig. 5b shows the same Teagasc soil map of raised peat bog in grey infill together with a second database (GSI Quaternary) mapping of peat in blue. The CLC18 land use classification of peat is shown in red. From Fig. 5b it is evident that the CLC18 database provides a significantly smaller area of classified peat than the other 2 databases which are mapping products. This is likely to be connected with the optical response of vegetation and tree cover in the land-use classification. Additionally, we note that a number of the peat polygons in both the Teagasc soil and GSI Quaternary databases are numerically identical. This aside, there remain considerable differences in the latter two peat databases. As noted by Beamish (2015), spatial inconsistencies in existing database descriptors of organic rich zones are common and the radiometric data can be used to assist in resolving such ambiguities. Fig. 5 a,b also show 3 rectangular areas (labelled A, M and S) which denote areas which are studied in detail later; these are retained in subsequent figures to assist with positional referencing.

3.8. Cutover and degraded raised peat bogs

From the 1700s onwards, the bogs were exploited as a source of cheap fuel. All the bogs in the study area are now classed as 'cutover' which indicates a degree of peat removal (and drainage modification) and an associated level of degradation. There are no known, routinely-available, relevant ground truth data for the peat areas considered. Commercial harvesting of some of the larger bogs (for power) commenced in the mid-20th century via the semi-state company Bord na Móna. Acknowledging the significance of the remaining carbon store contained in the bogs, all commercial exploitation has since ceased and a process of restoration and rehabilitation of many bogs is underway. Best practice in the restoration of raised bogs in Ireland is described by Mackin et al. (2017). Greenhouse gas emissions and balances from peat biomes in the UK and Ireland are discussed by Evans et al. (2021).

In order to convey the general form of the cutover raised bogs considered in the study area we use an illustrative example. The 4 × 4 km area selected (S in Fig. 5) is based solely on the availability of public-domain LIDAR topographic data. Four DTM (bare Earth) tiles (2 m

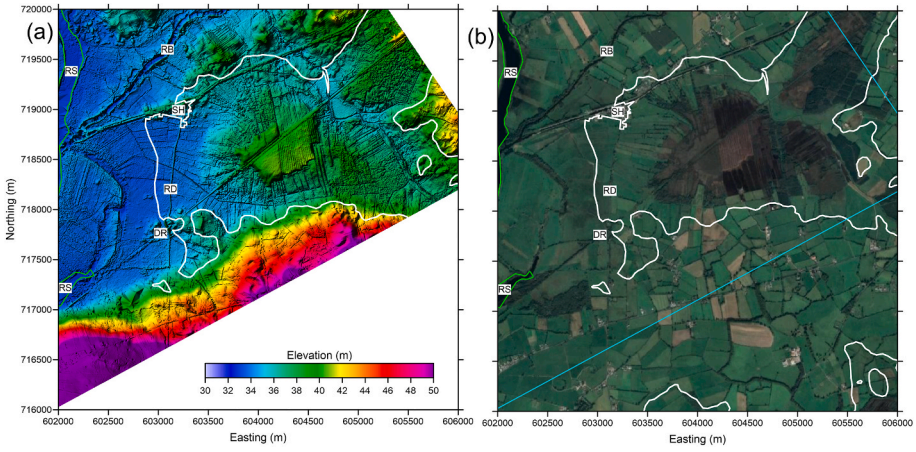

Fig. 6. A 4 × 4 km detailed study area (SH, Shannon harbour, Fig. 5) used to illustrate a modified and cutover raised peat bog. SH=Shannon Harbour (on Grand Union Canal). RS=River Shannon, RB=River Brosna. DR = Dismantled light-railway. The bog itself is defined within a cutover peat polygon (in white) from the Teagasc soil database. (a) Four DTM (bare Earth) elevation tiles (2 m resolution) using colour with shaded relief to highlight field boundaries, roads, tracks and cutover striations within the bog. (b) Google satellite image (©Google Earth) across whole area. (For interpretation of the references to colour in this figure legend, the reader is referred to the Web version of this article.)

resolution) are shown in Fig. 6a with shaded relief to highlight field boundaries, roads, tracks and cutover striations within the bog. The bog itself is defined within a cutover peat polygon (in white) from the Teagasc soil database. It can also be noted that no peat is detected within the optical CLC18 database (Fig. 5b). A satellite optical image across the full area is shown in Fig. 6b. The bog itself appears to be unnamed but lies to the SE of Shannon Harbour (SH) on the Grand Union Canal built to connect the Shannon (RS, Fig. 6) with Dublin.

All the raised bogs differ in their levels of modification but encroachment would have started at the perimeter and continued towards the centre (the high bog). Two separate areas of high bog remnants can be identified in both panels. Typically, in areas of high bog where the acrotelm is present the bog may be considered 'active' and capable of restoration (NPWS, 2014). The results across this area are presented later.

4. Results

4.1. Radiometric data and noise

The detailed technicalities of a particular airborne radiometric data set are not always addressed when the data are used for soil mapping purposes. It is useful to consider the main factors of elevation and associated field of view together with the likely signal/noise levels. The data sampling and altitudes of the 4 surveys contributing to the study are shown in Supplementary Material (Fig. SM4). The time/date stamping of the data is highly relevant when seasonal effects such as extremes of rainfall and flooding might be encountered. Survey operations are suspended in winter and during normal survey operations no acquisition is undertaken within several hours of a rainfall event.

Flights over water bodies provide a 'background null' or statistical noise level of the acquired and processed survey data. Data acquired, calibrated and processed precisely in the same way as the main data are preferred. Here we use over sea survey line data obtained in the west of survey block A2 (Fig. SM1). The radiometric noise levels obtained are defined and shown in Fig. 7. Here the figures are classified as 'indicative' as 4 different surveys are used across the study area and any large variations in survey altitude (atypical of over-water data) are not accounted for. The indicative noise level for the Total Count data is 14.4 cps.

The estimated noise levels become particularly significant when peat areas are studied; the attenuation provided by the low density/wet material is such that the noise level of the data may be encountered. Noise contributions are equally significant when, as here, spatial gradients of the data are employed and amplify the noise content. The contours of the noise levels within the peat are very extensive. In the case of the 3 individual radionuclides, the data across much of the peat would therefore be classified as random noise. In the case of the Total Count the noise level is encountered in the water body and is then much more spatially limited, being largely confined to a set of bogs in the north of the area (Fig. 7d).

For the attenuation assessment carried out here, the similar attenuation coefficients (Table 1) invariably give rise to equivalent

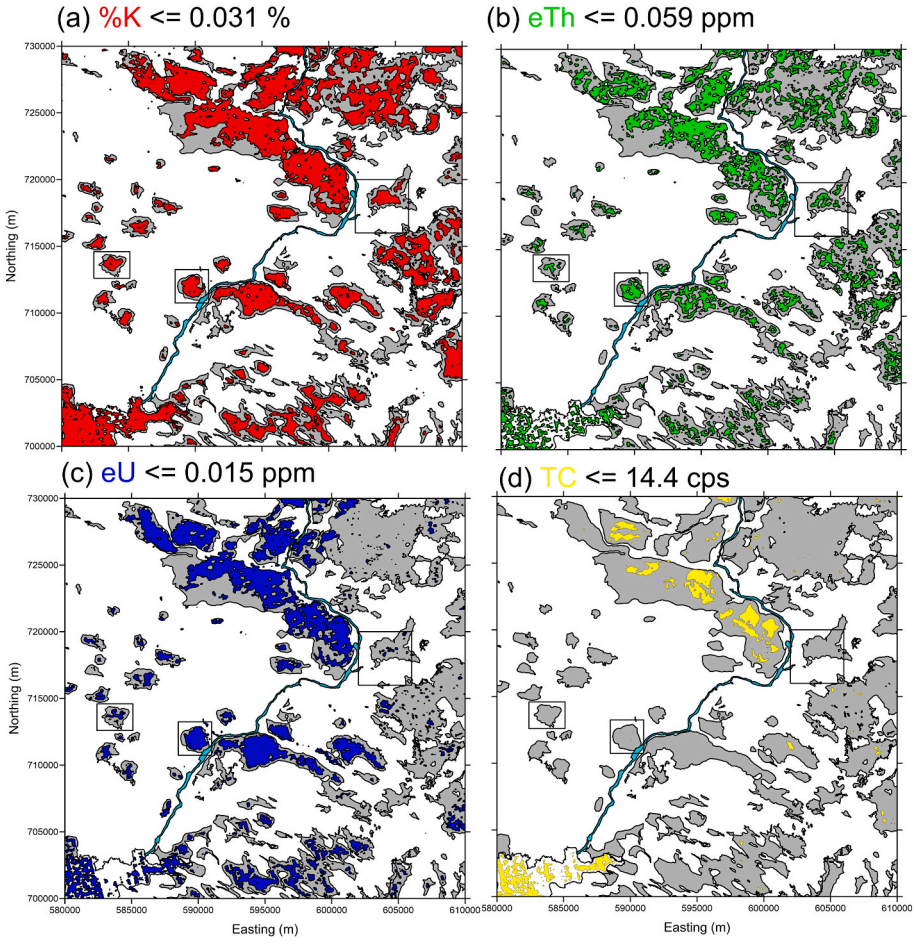

Fig. 7. Estimated indicative noise amplitudes of the survey data (infilled contours equal to and below the noise level) across the study area. (a) Potassium (%K). (b) Thorium (eTh). (c) Uranium (eU). (d) Total Count (TC). The estimated noise levels are tabulated in Table SM1. TEAGASC soil mapping of peat areas shown in grey infill. Shannon river in cyan. 3 rectangles are identified in Fig. 5. (For interpretation of the references to colour in this figure legend, the reader is referred to the Web version of this article.)

information. This has been verified by detailed assessments across the study area (not shown here). Beamish (2013) suggested that the most useful attenuation measurement is the Total Count (TC) which, being a spectral summation, offers enhanced signal/noise when examining low amplitude flux behaviour. Here, due to the spatially extensive noise of the 3 radionuclides across the survey area, we perform our analysis using only the Total Count data set.

Other amalgamated response metrics include dose rate (Beamish, 2014b) and sum normalisation which are both discussed in IAEA (2003).

4.2. Overview of soils in the study area

In the context of soil mapping, a specific soil type is detected/identified by a property contrast with adjacent soil types. As noted previously, here we use a simplified version of the soil database (Table 2) to allow a degree of interpretational control of the geophysical responses across the study area. The observed radiometric attenuation levels are essentially controlled by the bulk density/soil organic matter of each soil type if we initially assume a spatial uniformity in soil moisture. In the first instance we can summarise the differentials in the attenuation levels by performing a spatial join of the data with the soil database (e.g. Beamish, 2013). Fig. 8 shows the statistical behaviour of the soil classified TC data as a box-whisker plot. The low number of samples of the organo-mineral soils (classes C and D), confined to isolated small areas across the study area, can be noted. It is evident in Fig. 8 that the interquartile range of peat (F) is entirely separate and below those of all the other soils in the study area. This allows a unique identification of peat. The observed distribution displays a large skew to high values that is caused by misclassification, as demonstrated later. There is a progressive reduction in median values across the first 2 classes of mineral soils and then across the 2 classes of organo-mineral soils as BD reduces. It can be noted that the distributions of the well-drained and poorly-drained Brown Earth soils are very similar suggesting that there is no significant effect due to different moisture retention conditions. The alluvial soils display the largest range and we presume this relates to the presence of alluvial mineral soils in the upper quartile and alluvial organic soils in the lower quartile.

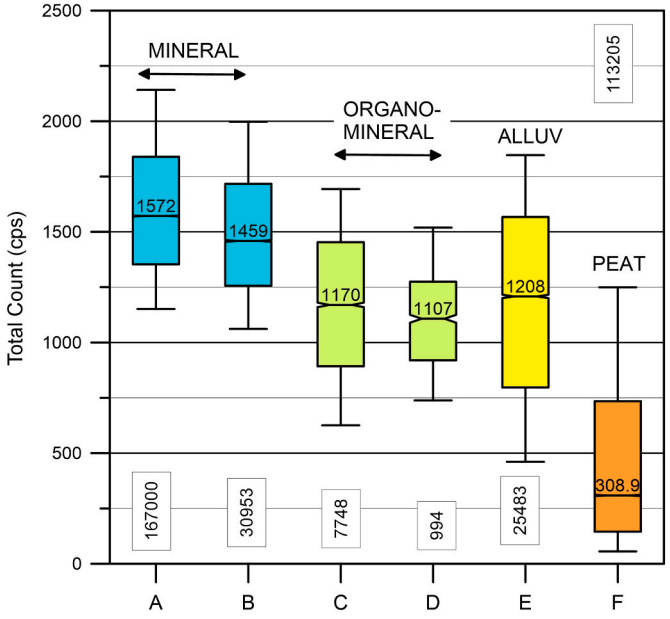

Fig. 8. Box and whisker plot summarising the statistical behaviour of the Total Count data classified according to the simplified version of the TEAGASC soil map with soil classifications from A to F (see Table 2). Vertical boxes give the number of data points, median values of the distributions are shown above each median bar.

4.3. Peat mapping and attenuation

Here we present the peat attenuation results across a series of 3 individual bogs (rectangles A, M, S in Fig. 5). We compare the geophysical (HGM) property contrast boundaries with the 3 peat control databases to assess accuracies although their inconsistent behaviour has been noted. We then summarise both the property-based HGM boundaries together with the attenuation levels across the whole study area, retaining the Teagasc soil mapping for reference.

4.3.1. Ardgraigue Bog (SAC)

The location of this bog (A) is shown in Fig. 5. This bog is representative of many of the isolated, small-medium size bogs. The bog is situated entirely within Brown Earth soils making it a particularly simple example. An SAC (Special Area of Conservation) report from 2003 notes that land use includes recent peat-cutting around most of the margins of the bog and reclaimed peat for agriculture to the north of the bog. Both activities have employed additional drainage. Here we use a study rectangle of 2.7 × 2 km to compare the cross-section of the previously modelled bog (Fig. 3) with the flux behaviour observed in practice.

Fig. 9a shows an optical satellite image with 2 polygons defining the area of mapped peat. The larger white polygon is from the Teagasc soil peat database while the smaller yellow polygon is from the Corine CEC18 database. The Quaternary peat polygon is numerically identical to that of the Teagasc polygon. The purely optical nature of the CEC18 surficial mapping of peat is evident in Fig. 9a and maps the vegetation contrast. Cut-over harvesting of peat (turf) is also evident around the margins of the bog.

Fig. 9b shows the contoured TC data which have a minimum value just above the indicative noise level. The main zone of attenuation (values of TC $<$ 1000 cps, say) has a perimeter of intense gradients clearly associated with the bog and a central uniform set of values (TC $<$ 200 cps) within the bog. The curvature-ridge analysis of Phillips et al. (2007) applied to the HGM response is summarised in Fig. 9c by the larger solid dots which allow a discrete form of the HGM edge detection to be compared with line-based soil mapping. This form of moving-window analysis can produce a level of spurious behaviour in the ridge solutions obtained. Here we retain only the highest amplitudes (HGM $>$3.5 cps.m^{-1}). In terms of peat mapping, the observational data indicate a broad correspondence with the 2 areas of mapped peat but also reveal subtle changes in the magnitude of the HGM response (defining the level of the property contrast) in the NW (a forested area) and in the SE.

The 2.7 km W-E cross-section (XS) of 5 radiometric responses is shown in Fig. 9d to allow a comparison with the theoretical response of Fig. 3. The 5 responses are individually scaled (from zero to a maximum value noted in the legend) to facilitate comparisons. The 3 radionuclides and TC data tend to a maximum several hundred meters beyond the mapped peat boundaries. The responses then decay to minima several hundred meters within the bog. The results are in agreement with the theoretical curves (Fig. 3) but on a larger lateral scale. The behaviour can be referred to as a lateral edge adjustment distance due to the 2D nature of a zone of discrete flux attenuation. The extent of the zone is mapped by the peak in the HGM response (the 'mapped' peat zone is not necessarily correct) as in Fig. 9b. Edge adjustment distances (internal and external) in the amplitude responses are of the order of 250 m. Within the bog a zone of uniform maximum attenuation is observed between 800 and 2000 m along profile. As noted previously, the 3 radionuclide responses are at or below the indicative noise levels (Fig. 7) but the TC response is relatively uniform and valid.

4.3.2. Meeneen Bog

The location of this bog (M) is shown in Fig. 5. This bog is again representative of many of the medium size bogs in the study area. The bog is situated within Brown Earth and alluvium soils and is bordered by

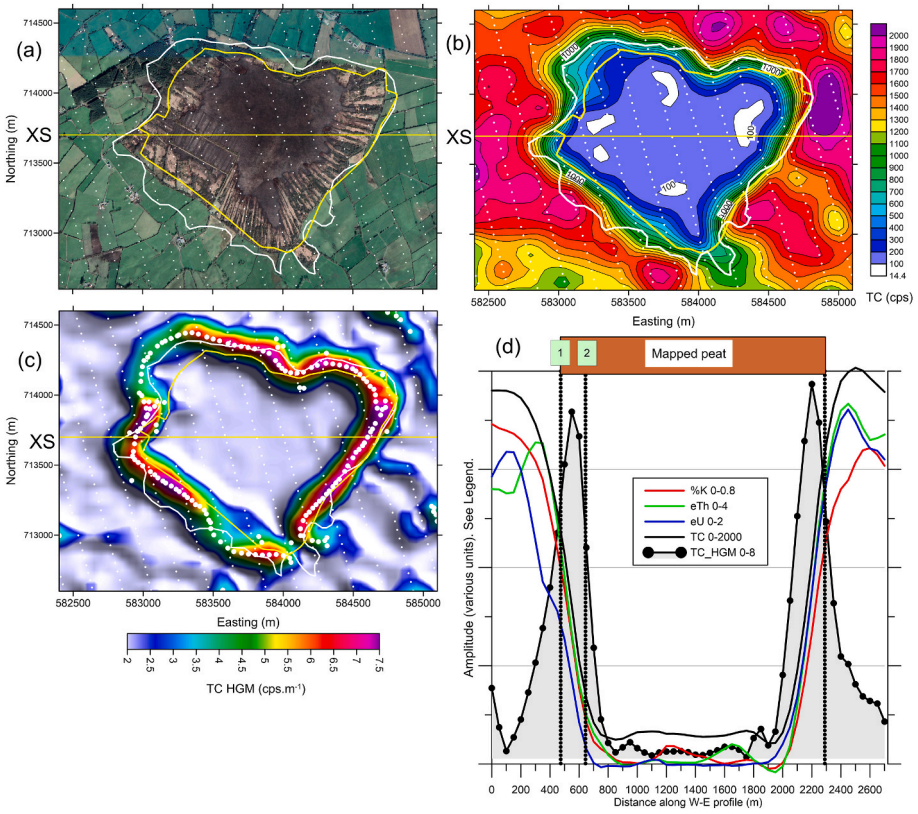

Fig. 9. Study of 2.7 × 2 km area centred on Ardgraigue Bog (A, Fig. 5). Small white dots are survey sampling points. XS refers to cross section in panel (d). (a) Google satellite image (©Google Earth) withwhitepolygon obtained from TEAGASC soil database, yellow polygon from CLC18 database.(b) Contours of Total Count (TC). (c) Image of TC HGM response (with shade). Heavy white dots show curvature ridge analysis with amplitudes >2 cps.m^{-1}. (d) Results along W-E cross section XS. All results are individually scaled as indicated in the legend using the plot maximum. TC HGM response is shown with grey infill. There are 2 mapped peat boundaries (1 & 2) in the west. (For interpretation of the references to colour in this figure legend, the reader is referred to the Web version of this article.)

the River Shannon in the SE. Here we use a study rectangle of 2.5 × 2.5 km. Fig. 10a shows a satellite optical image with 3 polygons defining the area of mapped peat. The larger white polygon is from the Teagasc soil peat database while the smaller yellow polygon is from the Corine CLC18 database. The Quaternary peat database is shown in dotted cyan and can be seen to overlay the majority of the white Teagasc polygon (except in the NE and in the south). Cut-over harvesting of peat (turf) is evident around the margins of the bog together with forested areas. Fig. 10b is from the simplified Teagasc soil map (Fig. 4) which defines a small area of poorly drained mineral soil (light brown) in the NE. A very small fragment/sliver of peat (white polygon) is also defined along the northern border.

Fig. 10c shows the TC data using an equal-colour histogram image with shade. The lowest amplitudes across the bog are just above the indicative noise level of 14.4 cps. An attenuation zone with an amplitude consistent with peat is observed in the NE, adjacent to the peat fragment. Fig. 9d presents the HGM curvature response of the TC data with ridge maxima that theoretically define any boundary contact points. Here we show the maxima with values of 1.5–3.5 cps.m^{-1} as white dots and values > 3.5 cps.m-1 as black dots. Overall, the HGM curvature response is clearly consistent with a quasi-circular form to the bog with reduced BD-SOM contrast in the east. In the NW the bog boundary is partially disrupted. The results of Fig. 10 c,d suggest a response in the NE that is consistent with a further peat response. A complex set of responses are observed in the SE in association with the bifurcation of the River Shannon. The flood plain encompasses the eastern and SE portions of the area (Fig. 5a). The potential consequences of persistent flooding of alluvial soils are referred to in the next example. The study illustrates the manner in which the property-based assessment is able to resolve significant differences in the 3 existing peat databases.

4.3.3. *Shannon Harbour Bog*

This far more complex and extensive (4 × 4 km) example was previously considered in Fig. 6 (Lidar and satellite optical data). Fig. 11a shows the Teagasc soil map (Fig. 4) across the area. Labels indicate the classifications of Table 2 that include mineral soils (A and B), organo-mineral soils (C), alluvium (E) and Peat (F). The Teagasc soil and Quaternary databases provide an identical mapping of peat. Fig. 11b shows the contoured TC data which have a minimum value of 71 cps well above the noise level of 14.4 cps. Assuming a uniform bedrock, the variations observed are all soil and water-course related. Statistically the only soil type that is detectable is that of peat (Fig. 8) and this is clearly observed in Fig. 11b. Attenuation zones are observed across the main central bog and a second area to the NE together with the peat zone identified in the SE corner. The main River Shannon along the western border provides a very clear attenuation zone along its length despite being only ~150 m wide. The river response acts as a useful 'control' for the study area. A final zone of similar attenuation is then observed in the west within an area classified as alluvium.

Fig. 11c shows the calculated HGM response coloured for values > 2 cps.m^{-1}. The form of the image response can be seen to trace the larger gradients present in the contours of Fig. 11b but additionally provides their magnitudes. Values > 7 cps.m^{-1} are associated with the control edges of the river and can be seen to define other 'strong' edges of the main bog particularly in the east. It is very evident that the western 'closure' of the main bog does not generate an edge response; this is associated with the gradational nature of the contours along the western zone of attenuation (Fig. 11b). Fig. 11d summarises the previous 3 panels with the HGM response replaced with the curvature-ridge analysis of the same data for values > 3.5 cps.m^{-1} (in cyan). Also shown is a single contour of the TC data (Fig. 11b) for a value of 900 cps (in blue);

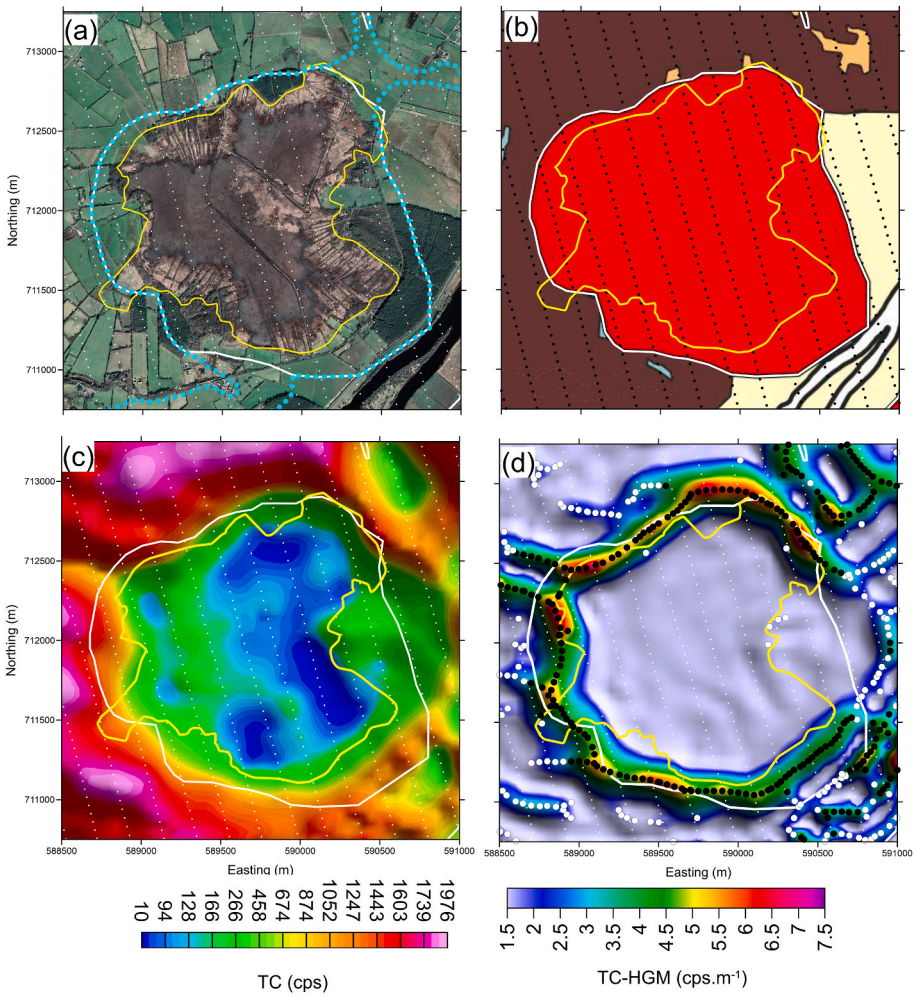

Fig. 10. Study of 2.5 × 2.5 km area centred on Meeneen Bog (M, Fig. 5). Small dots are survey sampling points. (a) Google satellite image (©Google Earth) withwhitepolygon obtained from TEAGASC soil database, yellow polygon from CLC18 database and dotted cyan is from the Quaternary peat database. (b) Soil map from TEAGASC soil map (Fig. 4) with 2 solid polygons from Panel (a). (c) Image of Total Count (colour histogram equalisation with shade) with 2 solid polygons from Panel (a). (d) Image of Total Count HGM response (with shade). Heavy dots show curvature ridge analysis with amplitudes 1.5 to 3.5 (white) and >3.5 cps.m^{-1} (black). 2 polygons from Panel (a). (For interpretation of the references to colour in this figure legend, the reader is referred to the Web version of this article.)

this value was chosen since it overlays the ridge results along the control provided by the river. In order to explain the lack of a strong western edge in the TC data we could advance a hypothesis that this due to the presence of organic alluvial soils to the west of the main bog. This seems unlikely given the statistical results of the 2 soil types (alluvium and peat) in Fig. 8. Instead, we suggest that the lack of a strong edge effect may be associated with a large area of persistent flooding across the floodplain to the east of the river (see Fig. 5a). We can refer to the detailed satellite study (Sentinel-1 data) of the unprecedented flooding of winter 2015–2016 that is located within the study area (O'Hara et al., 2019). Maps showing the kilometre range and persistence of the flooding events extend to the road (RD, Fig. 6) and eastwards into the bog. These winter floods are outwith the dates of survey data acquisition (Fig. SM4). Saint-Laurent et al. (2016) studied the influence of persistent flooding on the properties of alluvial soils and the modification of soil bulk density. Given the centuries of flooding events to the east of the river it is possible to conjecture that the such processes are responsible for the lack of an edge-effect (a property contrast) in these data although the attenuation level (Fig. 11d) still approximates the western boundary of the defined bog. We note that the effect is largely confined to this one instance as can be seen in the summary information across the whole study area presented in the next section. In Fig. 12b (next section) both the high attenuation zones and the HGM curvature-ridge analysis are compared and their ability to define peat-edges (as defined by mapping) can be evaluated. When examined in detail, it appears that the Shannon Harbour area is the one single, large-scale example of this effect observed across the study area. This suggests that both responses should, in general, be jointly examined in relation to the peat mapping objective.

The further separate zone of attenuation observed in the SW quadrant is also interpretationally problematic. The attenuation level is similar to that of peat and appears largely within alluvial soils. The response is quite distinct from the other alluvial soils and it may be a misclassification or a localised zone of highly organic alluvial material. The example shown illustrates the potential complexity of peat mapping, particularly in relation to cutover and modified raised bogs, using both attenuation and edge detection. It is evident that complex behaviour can be observed and a joint assessment of both aspects is recommended. In terms of the validation of the approach we note that the river (water) response provides a degree of local control and that the two responses (TC and HGM ridges) show a high degree of correspondence with the mapped boundaries of the 2 main areas of peat. They differ in detail (e.g. across the secondary bog in the NE) but are obtained on a property-based assessment of the material contrasts. We also note that when it comes to summarising the results across the whole study area, as presented below, we can expect attenuation and ridge features across non-peat areas. These are perfectly valid (in a signal/noise sense) but

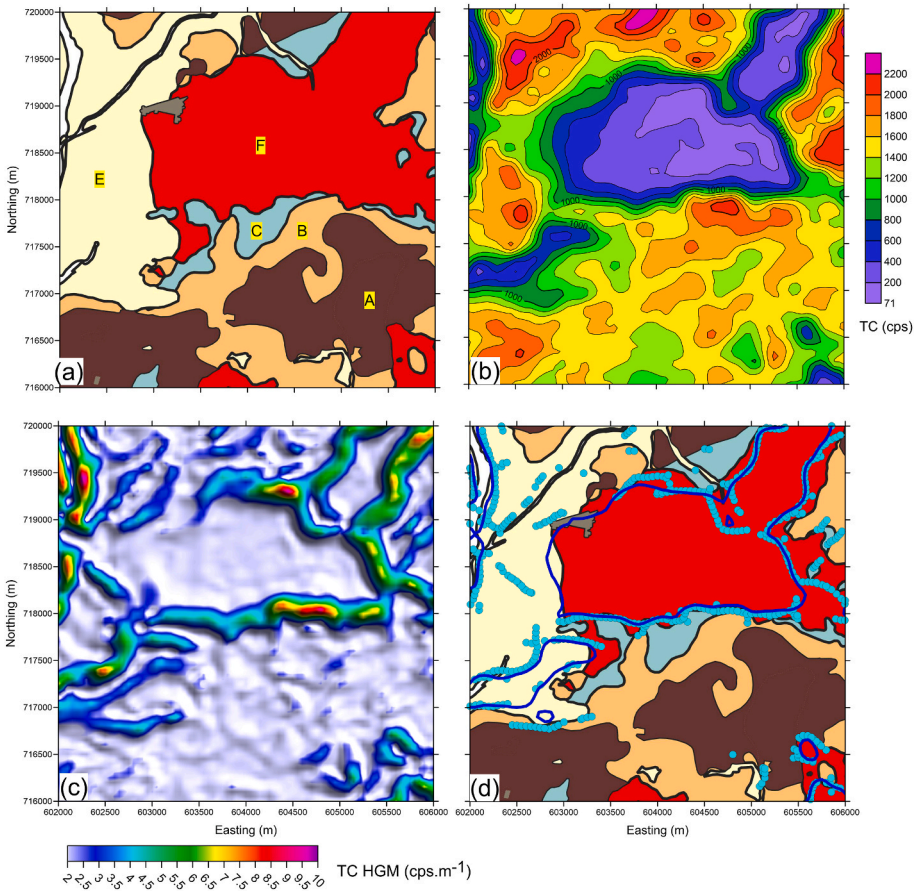

Fig. 11. Study of 4 × 4 km area referred to as Shannon Harbour (S, Fig. 5) see also Fig. 6. (a) Soil map from TEAGASC soil map (Fig. 4). River Shannon in white. Labels indicate soil classifications from Table 2. (b) The contoured TC data. (c) Image of Total Count HGM response for values > 2 cps.m^{-1}. (d) Combined results from previous panels. Heavy blue line is contour of TC = 900 cps (from panel b). Cyan dots show curvature ridge analysis of TC HGM data with amplitudes >3.5 cps.m^{-1}. (For interpretation of the references to colour in this figure legend, the reader is referred to the Web version of this article.)

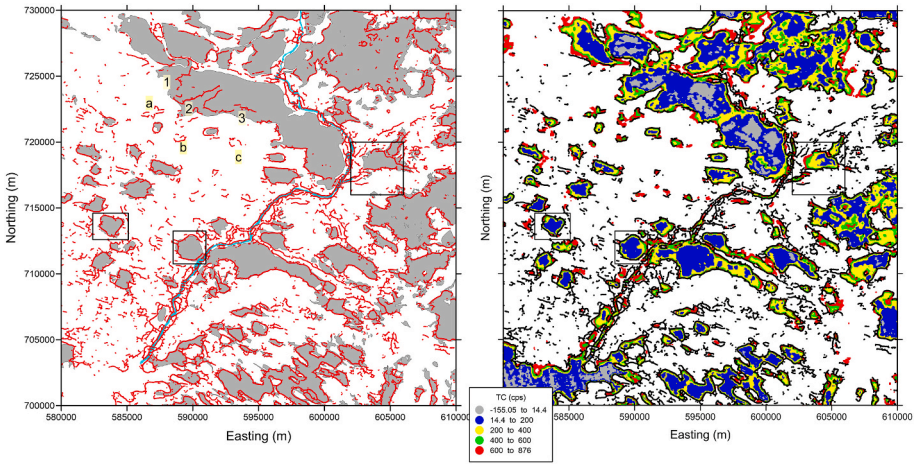

Fig. 12. Summary of results across the study area. 3 rectangles are identified in Fig. 5. (a) The HGM curvature ridge analysis applied to the Total Count HGM data. TEAGASC soil mapping of peat areas shown in grey infill. Shannon river in cyan. Red dots show curvature ridge analysis with amplitudes >3.0 cps.m^{-1}. Labels a to c and 1 to 3 are discussed in the text. (b) Summary of TC attenuation in relation to peat. All data (non-classified) showing values < 876 cps. The estimated TC noise level is 14.4 cps. The black dots are the curvature ridge analysis from panel a. The River Shannon is NOT shown explicitly. (For interpretation of the references to colour in this figure legend, the reader is referred to the Web version of this article.)

cannot be assessed unless examined at the detailed study scale.

4.3.4. Summary of HGM edge-detection and attenuation

The curvature-ridge analysis applied to the HGM response across all soils in the study area is shown in Fig. 12a. For simplicity we retain only the highest amplitudes (HGM >3 cps.m^{-1}) displayed in red. The Teagasc mapping of raised peat bog is shown by the grey polygons which, by their nature, typically form closures even at large scales. It is evident

that the detection of peat edges based on the behaviour of radiometric flux is broadly consistent with the mapped zones across the entire area and at all scales. The details and levels of the consistency have been provided in the 3 previous examples. We further note some of the behaviour observed in the NW quadrant. Three areas labelled 1 to 3 define large scale inconsistencies in the Teagasc peat soil database. These are also apparent in the differences between different peat databases (e.g. Fig. 5b). In addition, we note 3 small zones (a to c) whose partially closed form is suggestive of a raised bog, although classified as a Brown Earth soil. It is possible that these areas may be historically reclaimed for agriculture. The HGM ridge response, operating at the same amplitude level as a peat edge, is also observed across all the non-peat (largely Brown Earths) soils within the study area. Where spatially persistent they represent significant property contrasts.

For this data set it is possible to dispense with the existing soil database and simply plot the lowest amplitudes within the entire data set. A threshold of TC $<$ 876 cps provides attenuation zones that are generally consistent with the peat edge information contained in the HGM response. This approach removes the misclassification features within the soil database and relies only on observational geophysical information. Fig. 12b shows the posted-value plot of the low TC values. The attenuation zones thus defined appear largely consistent with the curvature-ridge information and allow the definition of numerous small zones of potential peat. At the site scale the intra-peat variations also allow assessments of the BD and soil moisture effects within individual bogs. Towards the margins of the peat zones a 'halo' effect is often apparent that is related to the edge adjustment distance discussed previously. The HGM curvature information can be considered more precise in defining a peat edge. In practice the precise HGM threshold used to define a peat edge is a matter of experimentation at the local scale since it is dependent on a number of factors e.g. the adjacent soil types together with signal/noise.

5. Discussion and conclusions

The detailed mapping of peat boundaries (raised bogs) using regional scale airborne radiometric data has been demonstrated both by modelling and by detailed studies at the local (individual bog) and at the regional scale. The lateral extent of peat has more significance than depth in the framework of carbon stock estimation. The technique employed uses a simple spatial derivative (the horizontal gradient magnitude, HGM) of the data together with a ridge detection procedure to define the boundaries of soil property contrasts. The analysis is conducted at the data grid resolution of 50 m. The technique applies to all soils but the largest contrasts are found in association with peat soils due to their distinctive high level of radiometric attenuation. The procedure is thus able to independently interrogate and clarify inevitable differences in existing peat mapping databases. Existing information on UK peat extent obtained using mapping techniques is discussed in IUCN (2023). The primary peat database used for comparisons (Teagasc soil) was also used as training data in the global model of peat extent developed by Melton et al. (2022). The suggested accuracy was 85% but the database is stated to be indicative due to the methods employed in its construction. It is also evident that a second peat database using optical satellite images (Corine, CLC18) to classify peat across this study area is strongly influenced by vegetation and tree cover. This gives rise to a significant underestimate of peat extent (Fig. 5b) in the case of the degraded bogs considered here.

Using the results obtained, the edge-detection method used in conjunction with an assessment of flux amplitude attenuation is recommended. According to the theoretical results of Fig. 3, an edge-detection analysis provides a precise location for the boundary of the property-contrast while, when using flux attenuation alone, an appropriate attenuation level (to define a boundary) must be assessed (it is therefore less precise). When examined in detail, the appropriate flux attenuation level is not known and may vary across individual peat bogs thus requiring a level of experimentation. In our whole area study (Fig. 12b) we have used the boundary obtained by edge-detection to define the *approximate* flux attenuation level (a single value) across all bogs.

Water bodies, including any wider river courses, provide a useful local control on the amplitude levels used in the interpretation. The intrinsic low lateral resolution of the observed data, a consequence of intrinsic edge-adjustment amplitude variations across soil property boundaries, has been demonstrated theoretically and empirically. The lateral edge adjustment distance is found to be of the order of 250m (both internal and external to the edge). The amplitude of the HGM response provides a consistent measure of the soil property contrast across a boundary. Attenuation levels observed within individual bogs may assist with their characterisation but theory suggests a low sensitivity to changes in bulk density. This is due to the dominant and distinct water saturation effect found in peat and 'peaty' soils (Fig. 1b). Indicative noise levels for this data set suggest that the 3 main radionuclides (Potassium, Thorium and Uranium) consist of random noise within much of the mapped areas of peat. The Total Count, used here, appears to avoid much of this effect.

The procedures described here identify edges associated with all the 128 peat bog polygons but an assessment of the accuracy of the results obtained is limited by differences that exist across the three available control peat databases. The property-based results based on both attenuation and edge-detection appear to resolve the mapping differences (both large and small). Additional areas of potential peat are also identified. In summary we suggest that the *property-based* mapping of peat (raised bogs) described here is reliable given good quality survey data.

There are two main recommendations generated by the study: (i) Although coarsely sampled spatially, more refined studies of the extensive Tellus soil radionuclide data set with regard to their detailed soil and bedrock classifications are recommended. (ii) We recommend extending the analyses conducted by van der Veeke et al. (2021) to obtain a more precise description of the depth contributions to each measurement at heights appropriate to existing airborne data sets (e.g. elevations from 50 to >200 m)

CRediT authorship contribution statement

David Beamish: Writing – original draft, Formal analysis, Conceptualization. **James C. White:** Writing – review & editing, Project administration.

Declaration of competing interest

The authors declare that they have no known competing financial interests or personal relationships that could have appeared to influence the work reported in this paper.

Data availability

The authors do not have permission to share data.

Acknowledgements

We thank Andy Tye for internal BGS reviewing. Three anonymous reviewers provided input to this final improved version of the manuscript. This research did not receive any specific grant from funding agencies in the public, commercial or not-for-profit sectors. This paper is published with the permission of the Executive Director, British Geological Survey (NERC).

Appendix A. Supplementary data

Supplementary data to this article can be found online at https://doi.

org/10.1016/j.jenvrad.2024.107462.

References

ADAS, 2019. Review of Best Practice for SOC Monitoring. Soil Policy Evidence Programme Report: SPEP 2019-20/05. Soil Policy & Agricultural Land Use Planning Unit, Land, Nature and Forestry Division. Department for Rural Affairs. Welsh Government. https://www.gov.wales/sites/default/files/publications/2021-04/review-best-practice-soil-organic-carbon-monitoring.pdf. (Accessed 17 February 2024).

Aitkenhead, M., Coull, M., 2019. Mapping soil profile depth, bulk density and carbon stock in Scotland using remote sensing and spatial covariates. Eur. J. Soil Sci. 71, 553–567. https://doi.org/10.1111/ejss.12916.

Beamish, D., White, J.C., 2011. A radiometric airborne geophysical survey of the Isle of Wight. Proc. Geologists' Assoc. 122 (5), 787–799. https://doi.org/10.1016/j.pgeola.2010.12.003.

Beamish, D., 2013. Gamma ray attenuation in the soils of Northern Ireland, with special reference to peat. J. Environ. Radioact. 115, 13–27. https://doi.org/10.1016/j.jenvrad.2012.05.031.

Beamish, D., 2014a. Peat mapping associations of airborne radiometric survey data. Rem. Sens. 6 (1), 521–539. https://doi.org/10.3390/rs6010521.

Beamish, D., 2014b. Environmental radioactivity in the UK: the airborne geophysical view of dose rate estimates. J. Environ. Radioact. 138, 249–263. https://doi.org/10.1016/j.jenvrad.2014.08.025.

Beamish, D., 2015. Relationships between gamma-ray attenuation and soils in SW England. Geoderma 259–260, 174–186. https://doi.org/10.1016/j.geoderma.2015.05.018.

Beamish, D., 2016a. Soils and their radiometric characteristics. In: Young, M.E. (Ed.), Unearthed: Impacts of the Tellus Surveys of the North of Ireland. Royal Irish Academy, Dublin. https://doi:10.3318/978-1-908996-88-6.ch19.

Beamish, D., 2016b. Enhancing the resolution of airborne gamma-ray data using horizontal gradients. J. Appl. Geophys. 132, 75–86. https://doi.org/10.1016/j.jappgeo.2016.07.006.

Billings, S., Hovgaard, J., 1999. Modelling detector response in airborne gamma-ray spectrometry. Geophysics 64, 1378–1392. https://doi.org/10.1190/1.1444643.

Carsten, P., Fealy, R., Fenton, O., Lanigan, G., O'Sullivan, L., Schulte, R.P.O., 2018. Assessing the role of artificially drained agricultural land for climate change mitigation in Ireland. Environ. Sci. Pol. 80, 95–104. https://doi.org/10.1016/j.envsci.2017.11.004.

Clymo, R.S., 1992. Models of peat growth. Suo 43, 127–136.

Connolly, J., Holden, N.M., Ward, S.M., 2007. Mapping peatlands in Ireland using a rule-based methodology and digital data. J. Soil Sci. Soc. Am. 71 (2), 492–499. https://doi.org/10.2136/sssaj2006.0033.

Connolly, J., Holden, N.M., 2009. Mapping peat soils in Ireland: updating the derived Irish peat map. Ir. Geogr. 42, 343–352. https://doi.org/10.1080/00750770903407989.

Creamer, R., Simo, I., O'Sullivan, L., Reidy, B., Schulte, R., Fealy, R.M., 2016. Irish Soil Information System: Soil Property Maps (2007-S-CD-1-S1). EPA Research Programme 2014–2020, EPA, Dublin. https://www.epa.ie/publications/research/land-use-soils-and-transport/EPA-RR-204-final-web.pdf. (Accessed 17 February 2024).

Creamer, R., O'Sullivan, L., 2018. The Soils of Ireland. Springer International Publishing, Cham, Switzerland. https://doi.org/10.1007/978-3-319-71189-8.

Cross, J.R., 1990. The Raised Bogs of Ireland, Ecology, Status and Conservation. Publication Office, Government of Ireland, Dublin. https://www.npws.ie/sites/default/files/publications/pdf/Cross_1990_Raised_Bogs.pdf. (Accessed 17 February 2024).

Duval, J.S., 1997. Gamma-ray Modelling Programs. U.S. Geol. Surv. Open File Rep, 97–96. http://pubs.usgs.gov/of/1997/of97-096/index.html. (Accessed 17 February 2024).

Duval, J.S., Cook, B., Adams, J.A.S., 1971. Circle of investigation of airborne gamma-ray spectrometer. J. Geophys. Res. 76, 8466–8470. https://doi.org/10.1029/JB076I035P08466.

Evans, C.D., Peacock, M., Baird, A.J., et al., 2021. Overriding water table control on managed peatland greenhouse gas emissions. Nature 593, 548–552. https://doi.org/10.1038/s41586-021-03523-1.

Fealy, R.M., Green, S., Loftus, M., Meehan, R., Radford, T., Cronin, C., Bulfin, M., 2009. Teagasc EPA soil and subsoils mapping project-final report. Volume I. Teagasc. Dublin. Available online: https://t-stor.teagasc.ie/.

Fortin, R., Hovgaard, J., Bates, M., 2017. Airborne gamma-ray spectrometry in 2017: solid ground for new development. In: Tschirhart, V., Thomas, M.D. (Eds.), Proceedings of Exploration 17: Sixth Decennial International Conference on Mineral Exploration, pp. 129–138.

Gallagher, V., Knights, K., Carey, S., Glennon, M., Scanlon, R., 2006. Atlas of Topsoil Geochemistry of the Northern Counties of Ireland. Geological Survey of Ireland. Ebook available at: https://www.gsi.ie/en-ie/publications/Pages/Geochemistry-Ebooks-Atlases.aspx.

Grasty, R.L., Minty, B.R.S., 1995. A Guide to the Technical Specifications for Airborne Gamma-Ray Surveys. AGSO Australian Geological Survey Organisation. Record 1996/60.

Grasty, R.L., 1997. Radon emanation and soil moisture effects on airborne gamma ray measurements. Geophysics 62, 1379–1385. https://doi.org/10.1190/1.1444242.

Hammond, R.F., 1979. The peatlands of Ireland. Soil Survey Bulletin 35. An Foras Talúntais, Dublin.

Heggeler, M.M.A., van der Ploeg, M.J., Vuurens, S.H., van der Schaaf, S., 2005. Subsidence of Clara Bog West and Acrotelm Development of Raheenmore Bog and Clara Bog East. Rapport/Wageningen University, Department of Environmental Sciences. Sub-Department Water Resources; No. 121). Sub-department Water Resources. https://edepot.wur.nl/212000.

Howie, S.A., Meerveld, I. Tv, 2011. The essential role of the Lagg in raised bog function and restoration: a review. Wetlands 31, 613–622. https://doi.org/10.1007/s13157-011-0168-5.

IAEA, 2003. Guidelines for Radioelement Mapping Using Gamma Ray Spectrometry. International Atomic Energy Agency, Vienna. Technical Report Series, No. 136.

IAEA, 2010. Radioelement Mapping. Nuclear Energy Series. International Atomic Energy Agency, Vienna (No. NF-T-1.3).

IUCN, 2023. Use of Peat Depth Criteria: Accounting for the Lost Peatlands. IUCN UK PEATLAND PROGRAMME. https://www.iucn-uk-peatlandprogramme.org/resources/briefings. (Accessed 17 October 2024).

Joint Nature Conservation Committee, 2011. Towards an assessment of the state of UK Peatlands. JNCC. https://hub.jncc.gov.uk/assets/f944af76-ec1b-4c7f-9f62-e47f68cb1050. (Accessed 17 February 2024).

Kiely, G., McGoff, N., Eaton, J., Leahy, P., Xu, X., Carton, O., 2009. SoilC – Measuring and Modelling of Soil Carbon Stocks and Stock Changes in Irish Soils. EPA, Dublin, Ireland. EPA report Strive No. 35, ISBN: 978-1-84995-320-6. https://www.epa.ie/publications/research/land-use-soils-and-transport/strive-35.php. (Accessed 17 February 2024).

Köhli, M., Schrön, M., Zreda, M., Schmidt, U., Dietrich, P., Zacharias, S., 2015. Footprint characteristics revised for field-scale soil moisture monitoring with cosmic-ray neutrons. Water Resour. Res. 51, 5772–5790. https://doi.org/10.1002/2015WR017169.

Lidman, F., Ramebäck, H., Åsa Bengtsson, Å., Laudon, H., 2013. Distribution and transport of radionuclides in a boreal mire – assessing past, present and future accumulation of uranium, thorium and radium. J. Environ. Radioact. 121, 87–97. https://doi.org/10.1016/j.jenvrad.2012.06.010.

Lindsay, R., 2010. Peatbogs and Carbon: a critical synthesis to inform policy development in oceanic peat bog conservation and restoration in the context of climate change. Environ. Res. Group Uni. East London. https://repository.uel.ac.uk/item/862y6. (Accessed 1 July 2023).

Løvborg, L., 1984. The calibration of portable and airborne gamma-ray spectrometers - theory. Problems and Facilities. Risø Report M-2456, p. 207.

Mackin, F., Barr, A., Rath, P., Eakin, M., Ryan, J., Jeffrey, R., Fernandez Valverde, F., 2017. Best Practice in Raised Bog Restoration in Ireland. Irish Wildlife Manuals, No. 99. National Parks and Wildlife Service, Department of Culture, Heritage and the Gaeltacht, Ireland. http://hdl.handle.net/2262/82140. (Accessed 17 February 2024).

Melton, J.R., Chan, E., Millard, K., Fortier, M., Winton, R.S., Martín-López, J.M., Cadillo-Quiroz, H., Kidd, D., Verchot, L.V., 2022. A map of global peatland extent created using machine learning (Peat-ML). Geosci. Model Dev. (GMD) 15, 4709–4738. https://doi.org/10.5194/gmd-15-4709-2022.

Minasny, B., Berglund, O., Connolly, J., Hedley, C., de Vries, F., Gimona, A., Kempen, B., Kidd, D., Lilja, H., Malone, B., McBratney, A., Roudier, P., O'Rourke, S.Rudiyanto, Padarian, J., Poggio, L., ten Caten, A., Thompson, D., Tuve, C., Widyatmanti, W., 2019. Digital mapping of peatlands - a critical review. Earth Sci. Rev. 196, 102870 https://doi.org/10.1016/j.earscirev.2019.05.014.

NPWS, 2014. Review of raised bog natural heritage area network. Nat. Parks Wildlife Serv. Depart. Arts Heritage Gaeltacht. Dublin. https://www.npws.ie/sites/default/files/general/national-raised-bog-sac-management-plan-en.pdf. (Accessed 17 February 2024).

O'Hara, R., Green, S., McCarthy, T., 2019. The agricultural impact of the 2015–2016 floods in Ireland as mapped through Sentinel 1 satellite imagery. Ir. J. Agric. Food Res. 58 (1), 44–65. https://doi.org/10.2478/ijafr-2019-0006.

Pitkin, J.A., Duval, J.S., 1980. Design parameters for aerial gamma ray surveys. Geophysics 45, 1427–1439.

Phillips, J.D., Hansen, R.O., Blakely, R.J., 2007. The use of curvature in potential-field interpretation. Explor. Geophys. 38, 111–119. https://doi.org/10.1071/EG07014.

Reinhardt, N., Herrmann, L., 2019. Gamma-ray spectrometry as versatile tool in soil science: a critical review. J. Plant Nutr. Soil Sci. 182 (1), 9–27. https://doi.org/10.1002/jpln.201700447.

Saint-Laurent, D., Paradis, R., Drouin, A., Gervais-Beaulac, V., 2016. Impacts of floods on organic carbon concentrations in alluvial soils along hydrological gradients using a Digital Elevation Model (DEM). Water 8, 208. https://doi.org/10.3390/w8050208.

Siemon, B., Ibs-von Seht, M., Frank, S., 2020. Airborne electromagnetic and radiometric peat thickness mapping of a bog in Northwest Germany (Ahlen-Falkenberger Moor). Rem. Sens. 12 (2) https://doi.org/10.3390/rs12020203.

Smyth, M., 1992. Geophysical Mapping Techniques to Investigate the Geological Structure of Two Raised Bogs, Clara and Raheenmore, Co. Offaly. AGP 92/2. Project Report Series, Applied Geophysics Unit. University College, Galway. https://www.npws.ie/sites/default/files/publications/pdf/Smyth_1992_Clara_and_Raheenmore_Bog.pdf. (Accessed 17 February 2024).

Tamponnet, C., Martin-Garin, A., Gonze, M.-A., et al., 2008. An overview of BORIS: bioavailability of radionuclides in soils. J. Environ. Radioact. 99 (5), 820–830. https://doi.org/10.1016/j.jenvrad.2007.10.011.

Van der Veeke, S., Limburg, J., Koomans, R.L., Söderström, M., de Waal, S.N., van der Graaf, E.R., 2021. Footprint and height corrections for UAV-borne gamma-ray spectrometry studies. J. Environ. Radioact. 231, 106545 https://doi.org/10.1016/j.jenvrad.2021.106545.

Young, M.E., 2016. The Tellus geoscience surveys of the north of Ireland: context, delivery and impacts. In: Young, M.E. (Ed.), Unearthed: Impacts of the Tellus Surveys of the North of Ireland. Royal Irish Academy, Dublin. https://nora.nerc.ac.uk/id/eprint/515341/.